Algorri, José Francisco; García-Cámara, Braulio; Urruchi, Virginia; Sánchez-Pena, José Manuel. (2015). High-Sensitivity Fabry-Pérot Temperature Sensor Based on Liquid Crystal Doped with Nanoparticles. *IEEE Photonics Technology Letters*, 27(3), pp.: 292-295.

DOI: https://doi.org/10.1109/LPT.2014.2369734

This article has been accepted for publication in a future issue of this journal, but has not been fully edited. Content may change prior to final publication. Citation information: DOI 10.1109/LPT.2014.2369734, IEEE Photonics Technology Letters

High-sensitivity Fabry-Perot temperature sensor based on liquid crystal doped with nanoparticles

J. F. Algorri, B. García-Cámara, V. Urruchi and J. M. Sánchez-Pena, *Senior Member, IEEE*

***Abstract*— The response of a Fabry–Perot interferometer filled with a nematic liquid crystal doped with silver nanoparticles is theoretically studied as a temperature sensor. It has been observed that the high dependence of the extraordinary refractive index of a liquid crystal along with the influence of the plasmonic resonances of nanoparticles produce useful phenomena for temperature sensing. Accordingly, we theoretically demonstrated the optical response of this device as a function of the temperature and the nanoparticles radius. The application of different technologies as optical sources was investigated through a simulation program. The latter enabled us to estimate the sensitivity and predict interesting parameters of the device, such as optimum wavelength ranges for the optical sources or optimum sizes of the nanoparticles. Maximum sensitivities of $24 \cdot 10^{-2}$ dB/ºC are obtained.**

***Index Terms* — Plasmons, Fabry-Perot interferometers, liquid crystals, effective medium theory, optical sensing and sensors.**

I. Introduction

Temperature is a sensitive parameter for many applications in various fields. Therefore, temperature sensors represent a wide range in the spectrum of sensor types. From the earlier thermistors to current optical fiber devices, there are many designs and models. The latter are highly appreciated in industry owing to their insensitivity to electromagnetic disturbances and easy integration. Most fiber-optic techniques for temperature sensing are based on phase or amplitude variations of a beam. Phase-based designs using interferometric configurations such as a Mach–Zehnder [1] or a Fabry–Perot (F–P) type [2] have been proposed. These devices are highly sensitive. However, they require conditioning circuitry or special equipment to measure the output signal (usually lambda shifts). On the other hand, amplitude-based devices use several physical phenomena such as light attenuation (quantum dots $1.6 \cdot 10^{-3}$ ºC^{-1} and $0.7 \cdot 10^{-3}$ ºC^{-1} [3]), frustration of total internal reflection (macrobend based on single mode silica fiber and sensitivities of $1.2 \cdot 10^{-2}$ dB/ºC [4], modified macro-bend loss with a multimode silica fiber and a sensitivity ranging from $1.5 \cdot 10^{-2}$ dB/ºC to $2.3 \cdot 10^{-2}$ dB/ºC [5], plastic optical fiber (POF) macrobend with a sensitivity of $1.29 \cdot 10^{-2}$ dB/ºC [6]), controlled mode coupling ($0.5 \cdot 10^{-2}$ dB/ºC) [7], light generation [8], films coatings in fibers ($13.4 \cdot 10^{-2}$ dB/ºC) [9] and fluorescence (fluorescence and glue with a multimode silica fiber and a sensitivity of $1 \cdot 10^{-2}$ dB/ºC [10]). Other studies have used other kinds of optical fibers, such as photonic fibers. The resulting sensitivity is around $3 \cdot 10^{-1}$ but the complexity of fabrication and use is increased [11]. The degree of complexity of these devices strongly depends on the specific configuration. Some of these sensors use the dependence of the refractive index of certain materials on temperature to act as transducers. Therefore, the use of nematic liquid crystals (NLCs) is very common for these applications owing to their high thermo-optic coefficients [12]. In fact, the thermo-optic coefficient (dn/dT) in NLCs is extraordinarily large, ranking among the largest of all known materials [13]. In addition, composites of liquid crystals doped with plasmonic nanostructures have emerged as interesting media for manipulating and improving the behavior of both the NLC and the nanoparticles (NPs) [14] [15] [16]. In particular, the interaction of light and metallic NPs (e.g. gold or silver) presents an interesting phenomenon known as Localized Surface Plasmon Resonance (LSPR) [17]. This phenomenon, which produces a strong enhancement of both the absorption and scattering of the NP, is currently used for a wide range of sensors. This change could be produced by the presence of an analyte, this is the case of plasmon-based biosensors [18], or by an active medium, such as liquid crystals [19]. The resulting composite has a strong alteration in the effective refractive index.

There are several works in the literature concerning the preparations and analysis of different mixtures of NLC and NPs, either metallic or semiconductor NPs [20]. These works reported the possibility to obtain homogeneous samples of colloid NPs in a NLC. Although the structure composition of the NLC, the size of these components with respect to the NPs as well as the local effect of the NPs into the NLC allows that some works consider the NLC as a homogeneous medium in which NPs are embedded [21].

In this paper, we propose the design of a temperature sensor based on an F–P resonator with a sensing element composed of an NLC doped with silver (Ag) NPs. The plasmon resonances of the NPs, which are affected by the temperature-dependent refractive index of the NLC, produce important changes in the effective refractive index of the composite, influencing the transmitted spectrum of the F–P. These

Manuscript received August 12, 2014; this work was supported in part by the Ministerio de Ciencia e Innovación of Spain (grant no. TEC2013-47342-C2-2-R) and the Comunidad de Madrid (grant no. FACTOTEM2 S2009/ESP-1781)

J. F Algorri, B. García-Camara, V. Urruchi and J. M. Sánchez-Pena are in the Electronic Technology Department, Carlos III University, Butarque 15, E28911 Leganés, Madrid, SPAIN (e-mail: jalgorri@ing.uc3m.es; vurruchi@ing.uc3m.es; jmpena@ing.uc3m.es).

This article has been accepted for publication in a future issue of this journal, but has not been fully edited. Content may change prior to final publication. Citation information: DOI 10.1109/LPT.2014.2369734, IEEE Photonics Technology Letters

variations in the transmitted power are used as the sensing principle in the proposed sensor. Additionally, this system takes advantage of the high sensitivity of an F–P configuration and the simplicity of amplitude measurements.

II. Structure and Operational Principle

An F–P interferometer, which is probably the simplest optical resonator, essentially consists of a plane-parallel plate of thickness l and refractive index n embedded between two flat mirrors. Light at the output interferes, producing both dark and bright fringes [22]. The maximum transmission, shown as bright fringes, is given by

$$\left|t_{\max}\right|^2 = \frac{(1-R)^2 e^{-2\alpha l}}{\left(1-R\,e^{-2\alpha l}\right)^2} \tag{1}$$

where R *is* the mirror's reflectance, and α is the absorption of the plate. Both the spatial position and intensity of the bright fringes strongly depend on the incident wavelength and on the thickness and refractive index of the plate. Thus, these interferometers are used for many applications such as spectrometers [23] or lasers [24]. In our system, the plate is made of a structured material or metamaterial consisting of an NLC doped with Ag NPs. This medium offers a high sensitivity to any variation in the temperature because of the high thermo-optic coefficient of the NLC. In addition, the variation in the refractive index of the NLC changes the scattering behavior of the Ag NPs. Both changes involve a strong alteration in the effective refractive index of the composite. These effects can be explained through the Maxwell–Garnet effective medium theory described in ref. [25]. In the referenced work, the effective permittivity of the medium is given by

$$\varepsilon_i' = \frac{\varepsilon_i\left[\varepsilon_i - L_i(\varepsilon_i-\varepsilon_m) - f(1-L_i)(\varepsilon_i-\varepsilon_m)\right]}{\left[\varepsilon_i - L_i(\varepsilon_i-\varepsilon_m) + f\cdot L_i(\varepsilon_i-\varepsilon_m)\right]} \tag{2}$$

where ε_i is the electric permittivity of the liquid crystal, both ordinary ($\varepsilon_\perp$) and extraordinary ($\varepsilon_\parallel$), and ε_m is that of the metallic NPs; f is the volume fraction of NPs in the composite, and L_i is the depolarization factor.

The temperature dependence of the refractive index of the NLC on both the temperature T and the incident wavelength λ are described by the Cauchy and extended Cauchy equations [26]:

$$n_i(\lambda) \cong A_i + \frac{B_i}{\lambda^2} + \frac{C_i}{\lambda^4} \tag{3}$$

$$n_i(T) \cong A - BT - \frac{(\Delta n)_0}{3}\left(1-\frac{T}{T_c}\right) \tag{4}$$

Δn and T_c are the birefringence and clearing point of the NLC, respectively. The coefficients (A_i, B_i, C_i, A, and B) of both equations are fitting parameters that should be estimated from experimental data [27].

The nanometric dimensions of Ag particles do not allow the use of their bulk properties owing to the motion of free electrons. Thus, the electric permittivity of Ag NPs has been deduced using the general Drude expression, given by [28]

$$\varepsilon(\omega) = \varepsilon_\infty - \frac{\omega_p^{\,2}}{\omega^2 + i\gamma\omega} \tag{5}$$

where ω is the angular frequency, ω_p is the plasma frequency of Ag, ε_∞ is a corrective constant that accounts for the background electron screening at high frequency, and γ represents the scattering frequency of the electron as it travels through the materials.

III. Results and Discussion

We have checked the behavior of the system by using several NLCs. This letter only presents results using an E7 and TL216 NLC, due to their high thermo-optics coefficient. The clearing point, defined as the temperature at which an LC converts to an isotropic liquid, is 58ºC for E7 and 80.3ºC for TL216. The extended Cauchy equations (4) of each NLC were estimated using the experimental data from ref. [27]. In addition, we considered both the ordinary and extraordinary refractive index of each NLC. However, while the temperature dependence of the extraordinary index is quite interesting, the effects of temperature on the ordinary refractive index are negligible. This indicates the need of any type of alignment layer that provokes a homogenous alignment. This is a very common process in the fabrication of LC devices. To avoid the rubbing process, different materials can be used (e.g. SiO_x or ZrO_2). The use of other materials, such as isotropic optical fluids (Acetone, Ethanol, etc) would avoid the use of

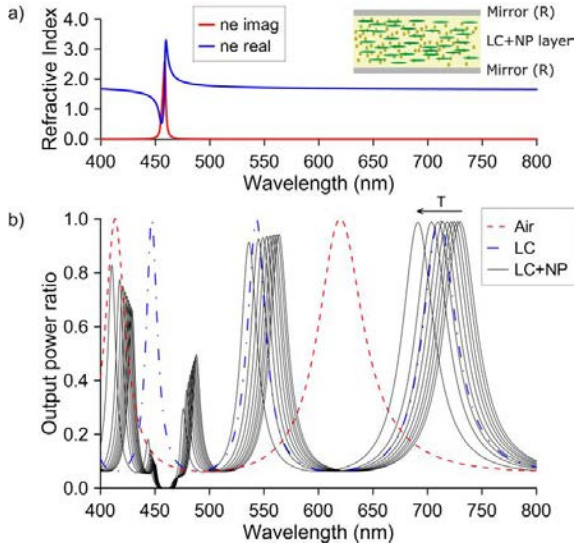

Fig. 1 (a) Effective refractive index of composite formed by E7 LC (extraordinary propagation) and 80nm-radius Ag NPs. (b) Output power ratio of F–P cavity filled with air (red dashed line), with E7 LC (blue dashed line), and with mixture of LC+Ag NPs (black line). Last curves are also plotted for several temperatures from 15 to 55 ºC; arrow shows the tendency.

This article has been accepted for publication in a future issue of this journal, but has not been fully edited. Content may change prior to final publication. Citation information: DOI 10.1109/LPT.2014.2369734, IEEE Photonics Technology Letters

alignment layers but reduce the sensitivity.

A. Proposal and response of the F-P sensor

After checking different values of the structural parameters, we considered those that can be used in real fabrication and yield a good response. For this case, a 0.62 μm cavity with a mirror reflectivity of 0.6 was filled with a mixture of NLC and a 0.01% volume concentration of Ag NPs. The necessary spacers are silica microspheres commercially available in the proposed size. Higher concentrations produce similar responses with more absorbance, and a homogeneous sample is harder to obtain. The mirrors of the F–P cavity can be of low quality because increasing the reflectivity increases the amount of absorption within it. This effect is caused by light rays rebounding in an absorbent medium.

The presence of plasmonic NPs in the F–P cavity produces interesting results for sensing. The refractive index of the composite (NLC+NPs) has the spectral profile shown in Fig. 1(a). The resonant behaviors associated with this profile produce two remarkable effects in the F–P cavity: high absorption at some specific wavelengths and an increase in the number of resonant modes in the considered spectral range. Fig. 1(b) compares the responses of an F–P cavity filled with air (red dashed line), with the NLC (blue dashed line), and with the composite NLC+NPs, in order to fully understand the different behaviors. Although the change from air to an NLC alone produces a spectral shift of the maxima, the composite produces a more complex spectrum. In particular, the inflection points of the real part of the composite's refractive index *n* cause the appearance of two new peaks (~450 nm and ~490 nm). The first is strongly affected by the absorption produced by the increase in the imaginary part of *n* and almost disappears. However, the second remains with an appreciable power ratio. All these peaks are strongly affected by any change in the temperature owing to the high thermo-optic coefficient of the NLC. The general behavior is that peaks are blue shifted and the power ratio decreases slightly as the temperature increases. Unlike other peaks, the new maximum at ~490 nm exhibits a strong dependence on the intensity, in contrast with a very small blue shift as the temperature increases. This effect, never associated with F–P cavities before, can be used to sense the temperature by light intensity measurements, and it is the basis of our design. Owing to the low required reflectivity in the F–P mirrors, the proposed sensor could be implemented simply by making a microcavity in the path of an optical fiber.

B. Study of several light sources

In our work, we considered four different technologies to sense the intensity change with the temperature in our design. All of them are commercially available, and the costs range from very low to moderate. The sensor output power ratio is estimated by convolution of the F-P and light source spectrums. The first study was done with an Argon-Ion laser (488 nm). Then a white light source and a 494/20 nm BrightLine® single-band bandpass filter from Semrock was used in the simulations. For the third study, a conventional green LED was used as a low-cost optical source. Finally, a commercial violet LED (LED405E, Thorlabs) was also used to test the range from 400 to 450 nm. In order to exploit the extraordinary refractive index one input polarizer would be necessary.

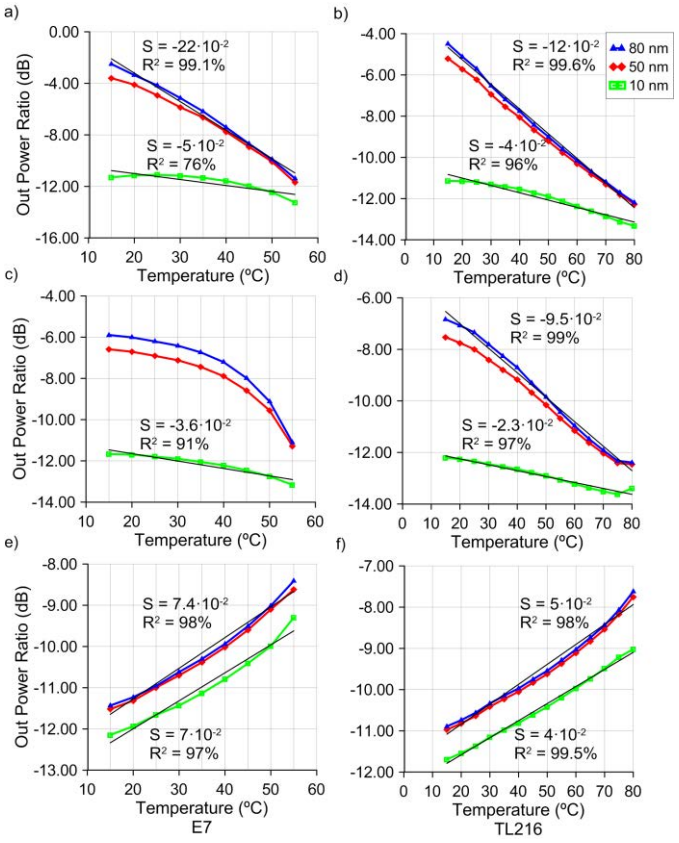

Fig. 2 Output power ratio (dB) of F–P interferometer for different LC (left E7 and right TL216), NP sizes in the composite and illumination technologies: (a) (b) 488 nm laser, (c) (d) optical filter, and (e) (f) conventional green LED.

Figure 2 shows the total output power ratio in decibels (for comparison with other works) considering the F–P response for the two NLCs. Three different sources and NP radius are shown. The results were fitted using the least squares approach. The linear regression coefficients (R^2) are also estimated. Different behaviors can be observed, mainly owing to the spectral range that these technologies cover. As explained above, the maximum sensitivity is expected in the F–P peak at ~490 nm. Thus, those technologies with narrower spectral bands will have the maximum sensitivities. Despite this, interesting results were found for specific technologies with a wide spectral range, for instance, a conventional green LED.

The commercial laser [Fig. 2(a) and (b)] gives the maximum sensitivities. Using 80 nm-radius Ag NPs yielded sensitivities of $22 \cdot 10^{-2}$ and $12 \cdot 10^{-2}$ dB/°C for E7 and TL216, respectively. This is about 10 times greater than the sensitivities of other related intensity sensors based on common fibers. In Fig. 2(c) the response is non-linear. This can be useful to obtain high sensitivities in certain temperature ranges. In Fig. 2 (e), using an inexpensive green LED as a light source, the maximum sensitivity, with 80 nm-radius Ag NPs, is still 5 times greater than those of other reported intensity sensors ($7.4 \cdot 10^{-2}$ dB/°C). Another important fact is the increase in sensitivity as the NP

This article has been accepted for publication in a future issue of this journal, but has not been fully edited. Content may change prior to final publication. Citation information: DOI 10.1109/LPT.2014.2369734, IEEE Photonics Technology Letters

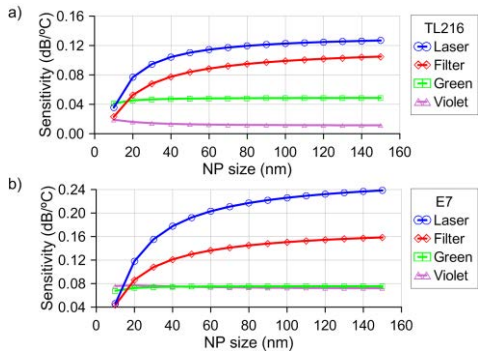

Fig. 3 Sensitivity (absolute value) of sensor as a function of NP radius for several optical sources and NLC compounds (a) TL216 and (b) E7.

size increases. Fig. 3 shows the results of a detailed study. This effect also depends strongly on the spectral range of the optical source. For the laser and optical filter, the NP size significantly affects the sensitivity because of the influence of NP plasmon resonances specifically located in the wavelength range of this optical elements (Fig. 3, blue and red line). In this sense, the sensitivity of the E7 increases from $4 \cdot 10^{-2}$ dB/°C (radius = 10 nm) to $24 \cdot 10^{-2}$ dB/°C (radius = 150 nm) [Fig. 3(b)]. In the case of the violet and green LED the wider spectrum produces a slight dependence of the sensitivity on the NP size. This can be considered an advantage because the NP size is no longer a critical parameter.

IV. Conclusion

In summary, an F–P cavity filled with an NLC doped with Ag NPs was theoretically analyzed. Different LCs, light sources and NP sizes were considered to optimize the model. The response curve of the sensor has high sensitivity and it is very linear for some cases. A maximum sensitivity of $24 \cdot 10^{-2}$ dB/°C was obtained using a laser source centered in the region affected by the plasmonic resonances of the NPs. This is about 10 times greater than other related intensity sensors based on common fibers. Despite this, the main advantage of the proposed sensor is the possible use with a light source of wide spectral range. As there is an overall reduction of the transmission spectra in the NP absorption region, the complete spectrum of the light source is attenuated. For a low-cost sensing application, a conventional green or violet LED yields sensitivities higher than other reported intensity sensors, based on silica or POF fibers.

References

[1] Khan, O. Krupinm, E. Lisicka-Skrzek, and P. Berini, "Mach-Zehnder refractometric sensor using long-range surface plasmon waveguides," Appl. Phys. Lett. vol. 103, pp. 111108, 2013.

[2] T. Zhu, T. Ke, Y. Rao, and K.S. Chiang, "Fabry-Perot fiber tip sensor for high temperature measurement," Opt. Commun. vol. 283, pp. 3683-3685, 2010.

[3] P. A. S. Jorge, M. Mayeh, R. Benrashid, P. Caldas, J. L. Santos, F. Farahi, "Quantum dots as self-referenced optical fibre temperature probes for luminescent chemical sensors," Meas. Sci. Technol., vol. 17, pp. 1032-1038, 2006.

[4] G. Rajan, Y. Semenova, and G. Farrell, "All-fibre temperature sensor based on macro-bend single mode fibre loop," Electron. Lett., vol. 44, pp. 1123-1124, 2008.

[5] G. Betta, A. Pietrosanto, "An intrinsic fiber optic temperature sensor," IEEE Trans. Instrum. Meas., vol. 49, pp. 25–29, 2000.

[6] A.T. Moraleda, C. V. García, J.Z. Zaballa, and J. Arrue, "A Temperature Sensor Based on a Polymer Optical Fiber Macro-Bend," Sensors, vol. 10, pp. 13076-13089, 2013.

[7] D.S. Montero, C. Vázquez, I. Möllers, J. Arrúe, D. Jäger, "A self-referencing intensity based polymer optical fiber sensor for liquid detection," Sensors, vol. 9, pp. 6446–6455, 2009.

[8] D. Hernandez, G. Olalde, A. Beck, E. Milcent, "Bicolor pyroreflectometer using an optical fiber probe," Rev. Sci. Instrum., vol. 66, pp. 5548–5551, 1995.

[9] J. Zhang, G. Liao, S. Jin, D. Cao, Q. Wei, H. Lu, J. Yu, X. Cai, S. Tan, J. Tang, Y. Luo, Z. Chen, "All-fiber-optic temperature sensor based on reduced graphene oxide," Laser Phys. Lett., vol. 11, no. 3, 2014.

[10] S. Tao and A. Jayaprakash, "A fiber optic temperature sensor with an epoxy-glue membrane as a temperature indicator," Sens. Actuator B: Chem., vol. 119, pp. 615-620, 2006.

[11] Y. Yu, X. Li, X. Hong, Y. Deng, K. Song, Y. Geng, H. Wei, and W. Tong, "Some features of the photonic crystal fiber temperature sensor with liquid ethanol filling," Opt. Express , vol. 18, pp. 15383-15388, 2010.

[12] E.P. Raynes, "Electro-optics and thermo-optic effects in Liquid Crystals," Phyl. Trans. R. Soc. Lond. A, vol. 309, pp. 167-178, 1983.

[13] J. Ptasinski, I. C. Khoo, Y. Fainman, "Passive Temperature Stabilization of Silicon Photonic Devices Using Liquid Crystals," Materials, vol. 7, pp. 2229-2241, 2014.

[14] O. Buchnev, J.Y. Ou, M. Kaczmarek, N.I. Zheludev, and V.A. Fedotov, "Electro-optical control in a plasmonic metamaterial hybridized with a liquid-crystal cell," Opt. Express, vol. 21, pp. 1633-1638, 2013.

[15] U. Singh, R. Dhar, R. Dabrowski, and M.B. Pandey, "Influence of low concentration silver nanoparticles on the electrical and electro-optical parameters of nematic liquid crystals," Liq. Cryst., vol. 40, pp. 774-782, 2013.

[16] J. Mirzaei, M. Urbanski, H.S. Kitzerow, and T. Hegmann, "Hydrophobic gold nanoparticles via silane conjugation: chemically and thermally robust nanoparticles as dopants for nematic liquid crystals," Phil. Trans. R. Soc. Lond. A, vol. 371, pp. 20120256, 2013.

[17] S.A. Maier, ed. Plasmonics: Fundamentals and applications, Springer 2007.

[18] J. Anker, W.P. Hall, O. Lyandres, N. C. Shah, J. Zhao, R.P. Van Duyne, "Biosensing with plasmonic nanosensors," Nature Mat., vol. 7, pp. 442-453, 2008.

[19] G. Z. Si, Y. Leong, E.S.P., Liu, Y.J. "Liquid-crystal-enabled active plasmonics: a review" Materials, vol. 7, pp. 1296-1317, 2014.

[20] Lysenko, D., Ouskova, E., Ksondzyk, S., REshetnyak, V., Cseh, L., Mehl, G.H. Reznikov, Y. "Light-induced changes of the refractive indices in a colloid of gold nanoparticles in a nematic liquid crystal" Eur. Phys. J. E., vol. 35, pp. 33, 2012.

[21] Wang, H., Vial,A. "Tunability of LSPR using gold-nanoparticles embedded in a liquid –crystal cell" J. Quant. Spectrosc. Radiant Transfer, vol. 146, pp. 492-498, 2014.

[22] P. Yeh, Optical Waves in Layered Media, Wiley& Sons, 1988.

[23] J. P. Carmo, R.P. Rocha, M. Bartek, G. de Graaf, R.F. Wolffenbuttel, and J. H. Correia, "A review of visible-range Fabry-Perot microspectrometers in silicon for the industry," Opt. & Laser Technol., vol. 44, pp. 2312-2320, 2012.

[24] K. Shi, F. Smyth, D. Reid, B. Roycroft, B. Corbett, F.H. Peters, and L.P. Barry, "Characterization of a tunable three-section slotted Fabry-Perot laser for advanced modulation format optical transmission," Opt. Commun., vol. 284, pp. 1616-1621, 2011.

[25] R.P. Devaty and A.J. Sievers, "Mie resonances for spherical metal particles in an anisotropic dielectric," Phys. Rev. B, vol. 31, pp. 2427-2429, 1985.

[26] J. Li and S.-T. Wu, "Extended Cauchy equations for the refractive index of liquid crystals," J. Appl. Phys., vol. 95, pp. 896-901, 2004.

[27] J. Li, C. Wen, S. Gauza, R. Lu, R. and S. Wu, "Refractive Indices of Liquid Crystals for Display Applications," J. Display Technol., vol. 1, pp. 51-61, 2005.

[28] J.A. Scholl, A.L. Koh, and J.A. Dionne, "Quantum plasmon resonances of individual metallic nanoparticles," Nature, vol. 483, pp. 421-427, 2012.